

## Chapter 6

### **The Transition between Anelasticity and Plasticity in Glass-Forming Metallic Liquids**

Amorphous metal, Elastic properties, Shear transformation zone, Ultrasonic measurement, Compression test, Glass, Enthalpy, Relaxation, Energy storage, Anelastic

#### **6.1 Abstract**

The relaxation processes of metallic glasses are investigated by observing the changes in material properties associated with the transient stress strain response of specimens subjected to isothermal deformations. The properties studied include the isoconfigurational shear modulus, configurational enthalpy, and the anelastic strain of the material. Conventional glass relaxation processes and Eshelby Stresses are applied to the description of the relaxations observed in the transient response of the material. Additionally, the criteria for shear localization and the barrier height controlling flow are investigated using steady-state flow properties of the material at different strain rates.

## 6.2 Introduction

In traditional crystalline metals extensive thermoplastic heating occurs. Most metals have a dissipation coefficient of  $f_d \approx 0.9$  for the conversion of input mechanical work into heat [1]. Here,  $f_d$  is the fraction of mechanical inelastic work dissipated as heat during deformation. Bruck et. al. performed a series of high-strain-rate experiments at room temperature utilizing a Kolsky Bar setup and an infrared temperature sensor to measure the dynamic compressive behavior of bulk metallic glasses. Metallic glasses at ambient T deform by shear banding, as opposed to the homogeneous mode of deformation common in crystalline metals. This gives rise to several interesting phenomena. It was observed that the yield stresses of the metallic glasses were invariant to the strain rates used. Furthermore, in contrast to traditional metals, no measurable adiabatic heating of the material is observed before inhomogeneous deformation occurs. After inhomogeneous deformation is initiated a large thermal release of energy is observed in the activated localized shear bands during flow. It was estimated that the temperatures within the shear bands may approach that of the alloy melting temperature. This would explain the river like morphology observed on the fracture surfaces of metallic glasses [2].

Since the crystallized glass represents true equilibrium, it should be noted that all glasses are in a non-equilibrium state. The glass is in a metastable state which is the extension of the liquid into the undercooled liquid regime. As the temperature is lowered towards the glass transition, the relaxation time of the undercooled liquid grows rapidly. On any laboratory time scale, the liquid falls out of equilibrium below some “freezing” temperature. The quenched glass at ambient temperature is frozen in a liquid

whose atomic configuration is characteristic of the temperature where it fell out of equilibrium. This is often referred to as the “fictive” temperature of the frozen glass. The state of the glass is thus dependent on its history.

By annealing a glass for long times compared to the relaxation time at a temperature near  $T_g$ , the glass can be relaxed to the equilibrium state at the respective temperature. Thus, one can refer to such glasses as relaxed or equilibrated liquids at the specified annealing temperature. Likewise, at a given  $T \sim T_g$ , we can define equilibrium and non-equilibrium glasses.

It is through relaxation processes that glasses approach their equilibrium energy states. It has been proposed that there are two types of relaxation processes for conventional glasses. Most conventional glass theories describe an irreversible  $\alpha$  process that is preceded by an anelastic  $\beta$  process. Predominately, the  $\beta$  process is viewed as being a locally initiated process and the  $\alpha$  process is a large-scale irreversible rearrangement of the material [3-6]. The view of  $\beta$  preceding the irreversible  $\alpha$  process is supported by an earlier work of Orowan [7] in which he describes that a single rearrangement alone is never an irreversible process of flow, but can at best be a retarded recoverable elastic deformation. In addition to the dielectric methods used by Johari et. al. [4-6], mechanical creep and nanoindentation studies have been used to probe the transition between the anelastic  $\beta$  response and the plastic  $\alpha$  response [8-12].

In a series of studies by Argon et. al. a systematic study of the anelastic “creep recovery” response of metallic glasses was undertaken [10-12]. The experimental setup involved torsional specimens that were subjected to creep at elevated temperatures for a preset amount of time. After the creep tests under torsional load, the specimens were

subjected to annealing treatments to relax the anelastic strain which was presumed to be stored in the samples. By doing the relaxation at different temperatures for the same time increment Argon was able to obtain an activation energy distribution for the relaxation processes associated with the anelastic response. Argon proposed that the observed anelastic response was due to mechanically polarized areas within the material returning to their original configurations when relaxed at elevated temperatures. Furthermore, each mechanically polarized region will have an associated stress field. The model developed by Eshelby may be used to approximate the compatibility stresses arising when the polarized regions are confined by the surrounding unpolarized matrix. The derivation for the Eshelby analysis can be found in Refs. [13, 14]

More recently, in the Cooperative Shear Model developed by Johnson and Samwer [15], a Frenkel-like potential was applied to a fold catastrophe in metallic glasses. Using a temperature analysis of the yield criterion for different metallic glasses, a critical strain to the yield point was obtained. Using this analysis the potential energy landscape was related to the elastic properties of these materials. Recent studies have used acoustic experiments along with density measurements to evaluate changes in the isoconfigurational shear modulus of fully relaxed samples with respect to temperature [16]. Additionally, there are experiments relating the viscosity of the material during steady-state deformation with the energy of the system and the isoconfigurational shear modulus [17, 18].

The motivation for this chapter is the application of conventional glass relaxation processes and Eshelby Stress Fields to the description of metallic glasses. We hope to probe the relaxation processes of metallic glasses by observing the responses related to

the shear modulus, stored configurational enthalpy, and anelastic strain during the transient stress strain response of the material. Additionally, the criteria for shear localization and the barrier height controlling flow are investigated using data obtained from steady-state flow measurements of the material at different strain rates and varying temperature.

## 6.3 Experimental

We utilized 6 mm diameter cast cylindrical rods of  $\text{Pd}_{43}\text{Ni}_{10}\text{Cu}_{27}\text{P}_{20}$  [19] that were annealed and structurally relaxed at 548 K for 48 hr prior to testing. After being structurally relaxed the 6 mm diameter rods were sectioned into 9 mm lengths. The 1.5 to 1 ratio was used to enable a clearer acoustic signal. The specimens were compressed at 548 K and a constant strain rate of  $10^{-4} \text{ s}^{-1}$  using the set-up described in Ref. [20]. The specimens were deformed to different total strains in order to evaluate the properties of the material during the transient stress strain response. Additionally, the steady-state response of the system at different strain rates was investigated by evaluating the properties of specimens deformed at 548 K and strain rates ranging from  $5 \times 10^{-6} \text{ s}^{-1}$  to  $10^{-4} \text{ s}^{-1}$ . In all cases, upon unloading the specimens were quenched as rapidly as possible in order to capture the configurational state associated with the deformation at 548 K.

We assessed the elastic softening induced by mechanical deformation by evaluating the isoconfigurational shear modulus at a high-frequency “solid-like” limit,  $G$ . We evaluated  $G$  of the quenched unloaded specimens by utilizing ultrasonic measurements along with density measurements at ambient temperature [21]. We subsequently corrected the room-temperature measurements to estimate  $G$  at the temperatures of the flow experiments by accounting for the thermal expansion (Debye-Grüneisen) effect on the shear modulus of the frozen glass, as discussed in Chapter 4. Shear wave speeds were measured using the pulse-echo overlap setup described in Ref. [16]. Densities were measured by the Archimedes method, as given in the American Society for Testing and Materials standard C693-93.

We assessed the configurational changes induced during mechanical deformation by evaluating the configurational enthalpy stored in the deformed specimens,  $\Delta h$ , as measured using Differential Scanning Calorimetry (DSC) [22] at a scan rate of 10 K/min. We take  $\Delta h$  to be the change in the recovered enthalpy with reference to a specimen relaxed at 548 K with no imposed deformation. The absolute values for the recovered enthalpy in this chapter are not directly comparable to those obtained in Chapter 5. This is due to a new head being installed on the DSC between the respective studies. This necessitated a new reference curve being obtained from a different calibration curve.

We have evaluated the anelastic response of this metallic glass at different total strains by annealing the quenched unloaded specimens at 558 K for 4 hr. Before and after the annealing treatment the specimen heights were measured using calipers with an accuracy of  $\pm 0.005$  mm. The height measurements were used to evaluate the specimen plastic strain state before and after annealing. Samples subjected to additional annealing treatments showed no measurable increase in the total strain recovered. This confirmed that the 4 hr annealing was sufficient to determine the maximum recoverable strain. The amorphous nature of the specimens after the annealing process was confirmed using x-ray diffraction. The reference sample annealed and relaxed at 548 K showed no measurable length change after the annealing process at 558 K.

For a more detailed account of specimen preparation, mechanical testing, and the property evaluation techniques used please see the experimental sections in Chapters 2.3 and 5.3.

## 6.4 Discussion

In Fig. 6.1 we present the different stress-strain curves obtained. The total strains measured range from  $\varepsilon_T = 0.010$  to  $\varepsilon_T = 0.204$ . The inelastic mechanical work,  $W$ , done on the specimens was taken as the area under the stress-strain curves minus the elastic energy. Only the inelastic mechanical work was taken because the elastic energy stored in the material is completely recovered at the end of deformation. The elastic energy was estimated as  $\frac{1}{2} \frac{\sigma^2}{E}$ . We take  $\sigma$  to be the normal shear stress and  $E$  to be the Young's Modulus for a reference sample relaxed at 548 K.  $E$  was acoustically measured to be 87.05 GPa.  $E$  was assumed to be constant for the elastic energy correction.

In Fig. 6.2  $\Delta h$  initially increases linearly with increasing  $\varepsilon_T$ . As steady state deformation is approached  $\Delta h$  relaxes to a constant value. This steady state value is obtained in the region of  $\varepsilon_T \sim 0.105$ . This transition to steady state at  $\varepsilon_T \sim 0.105$  is in agreement with the predicted distance between configurations derived in Johnson et. al. [15]. In Fig. 6.3  $G$  is observed to linearly decrease as  $\Delta h$  increases in Fig. 6.2. This trend is in agreement with Refs. [18, 23]. Furthermore,  $G$  approaches steady state at the same  $\varepsilon_T$  as  $\Delta h$ . All of the observations confirm that the sample reaches a well-defined uniform steady-state flow following an initial transient response. Furthermore, it shows that both the shear modulus,  $G$ , and stored configurational enthalpy,  $\Delta h$ , relax on the same time scale to a unique steady-state value.

Prior to steady-state deformation there is a highly efficient conversion of mechanical work,  $W$ , into stored configurational enthalpy,  $\Delta h$ . Moreover, the conversion of  $W$  into  $\Delta h$  is nearly one to one during the initial stages of deformation. Once steady



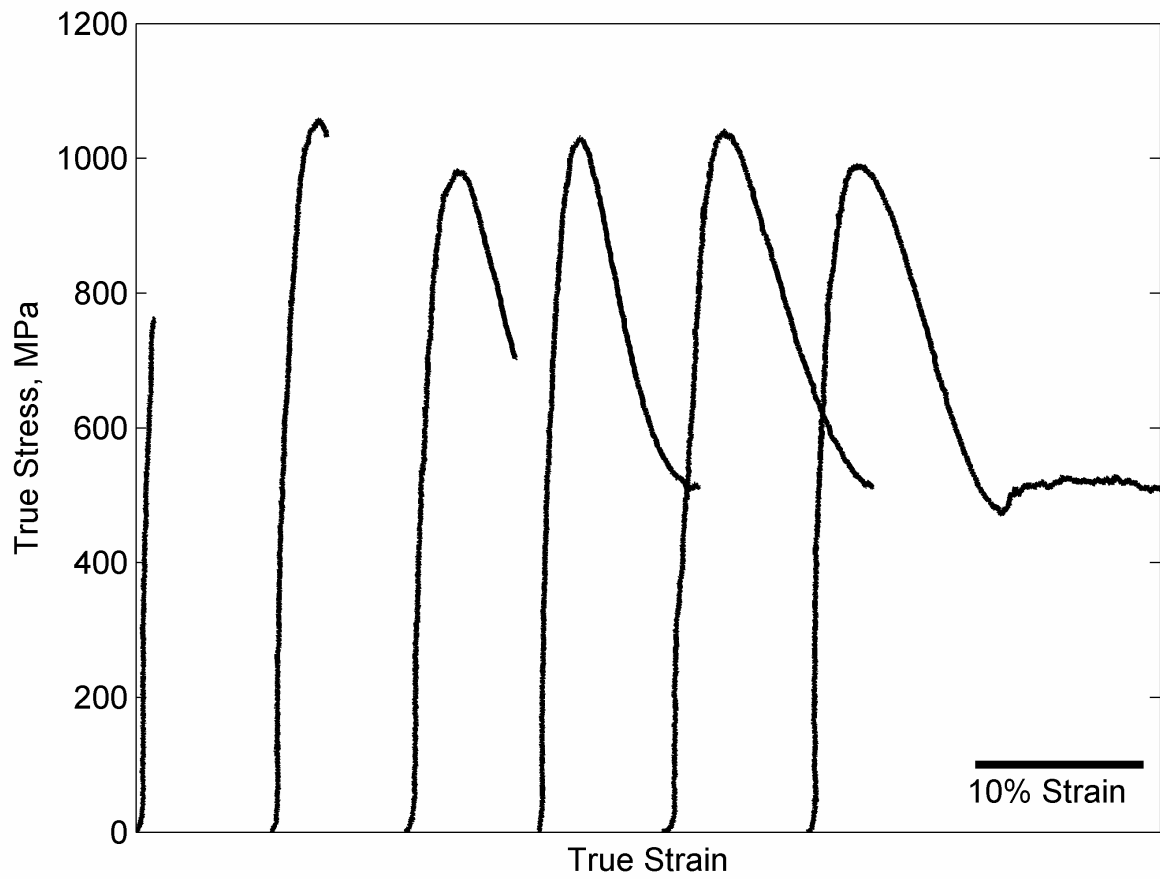


**Figure 6.1.** True stress versus true strain for Pd<sub>43</sub>Ni<sub>10</sub>Cu<sub>27</sub>P<sub>20</sub> samples deformed at 548 K and  $10^{-4} \text{ s}^{-1}$ . The specimens were deformed to different total strains up through steady state.

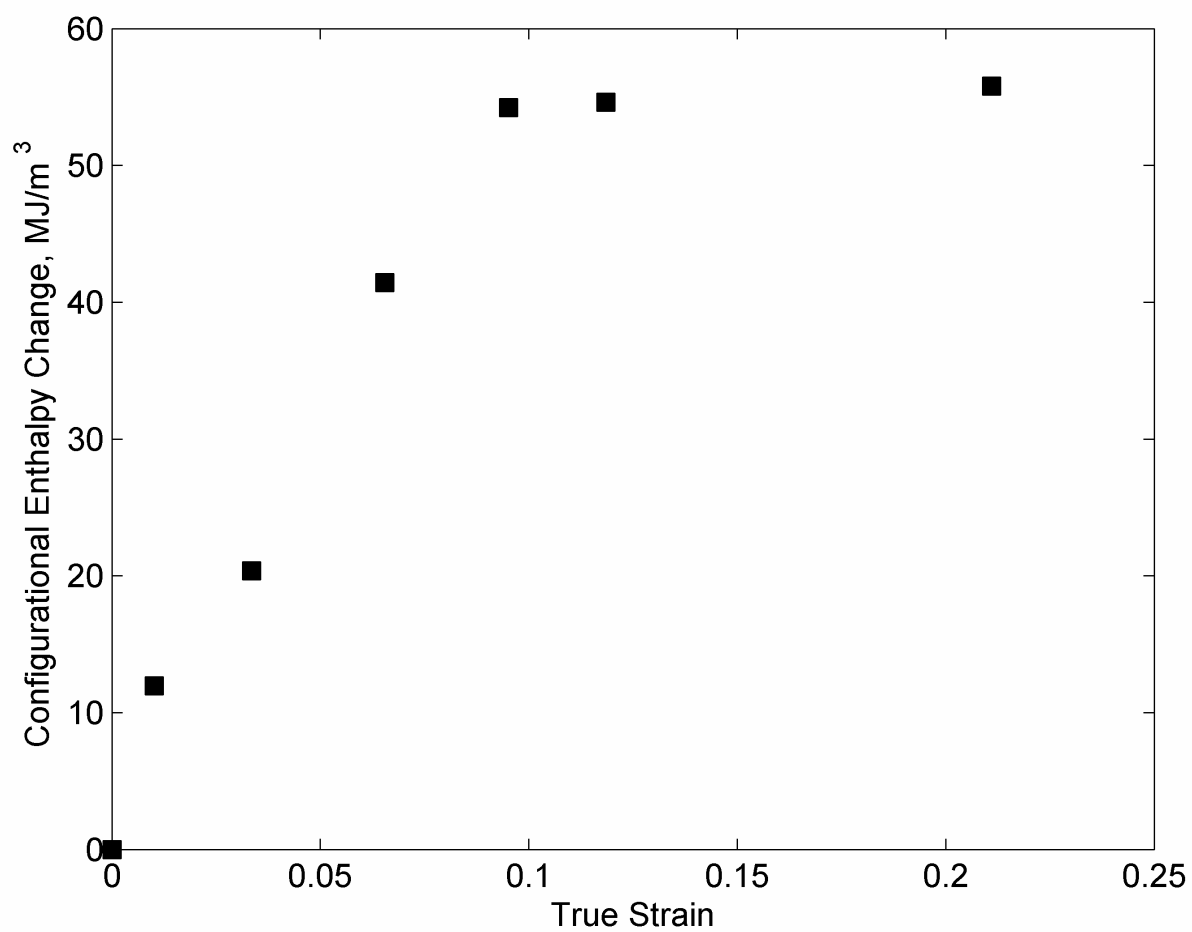


**Figure 6.2.** Configurational enthalpy for the quenched unloaded Pd<sub>43</sub>Ni<sub>10</sub>Cu<sub>27</sub>P<sub>20</sub> specimens as measured with Differential Scanning Calorimetry at a scan rate of 10 K/min versus true strain

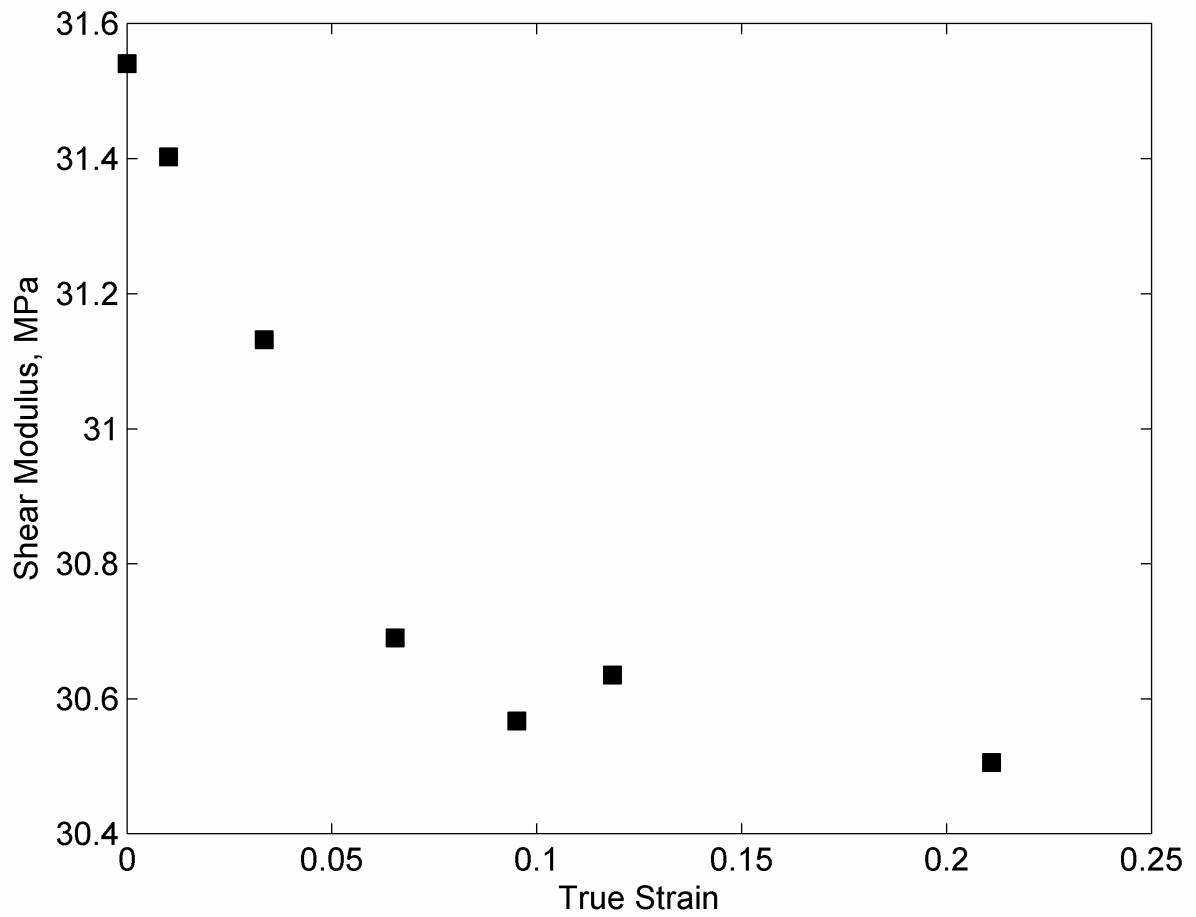


**Figure 6.3.** Acoustically measured shear moduli (corrected for Debye-Grüneisen effect) of the quenched unloaded Pd<sub>43</sub>Ni<sub>10</sub>Cu<sub>27</sub>P<sub>20</sub> specimens versus true strain

state is obtained no further changes are observed in  $\Delta h$ . Therefore, additional mechanical work input into the system upon reaching steady state is completely dissipated as heat. This transition from an efficient energy storage process to a completely dissipative process can be seen in Fig. 6.4.

The anelastic strain response of the material is shown in Fig. 6.5 as the percentage of inelastic strain that was recovered after the quenched unloaded samples were subsequently annealed. The remaining fraction of inelastic strain can be directly contributed to irreversible plastic deformation. At strains prior to the transient peak stress the deformations appear to be completely recoverable. At strains corresponding to or greater than the peak stress the fraction of recoverable strain is found to decrease. In the limit of large strains the fraction of recoverable strain becomes insignificant.

Drawing on the work of Johnson et. al. [15] and Argon et. al. [10-12] it is possible to propose a physical description of what is occurring in the material during deformation. Argon et. al. put forward that mechanically polarized regions within the material were responsible for the anelastic behavior observed. Johnson et. al. utilized a cooperative shear model to describe the deformation of metallic glasses. An analogy may be drawn between these two models and the anelastic  $\beta$  process preceding the irreversible  $\alpha$  process described in Refs. [3-6] for conventional glasses.

Before deformation there should be a random distribution of internal stress fields within the material. Once an external stress field is applied, local reorientations, which we will call “ $\beta$  buckle ups”, will occur to accommodate that stress. This results in mechanically polarized regions within the material. These  $\beta$  buckle ups will be subject to an Eshelby Stress Field that is due to the constraint of the polarized regions confined

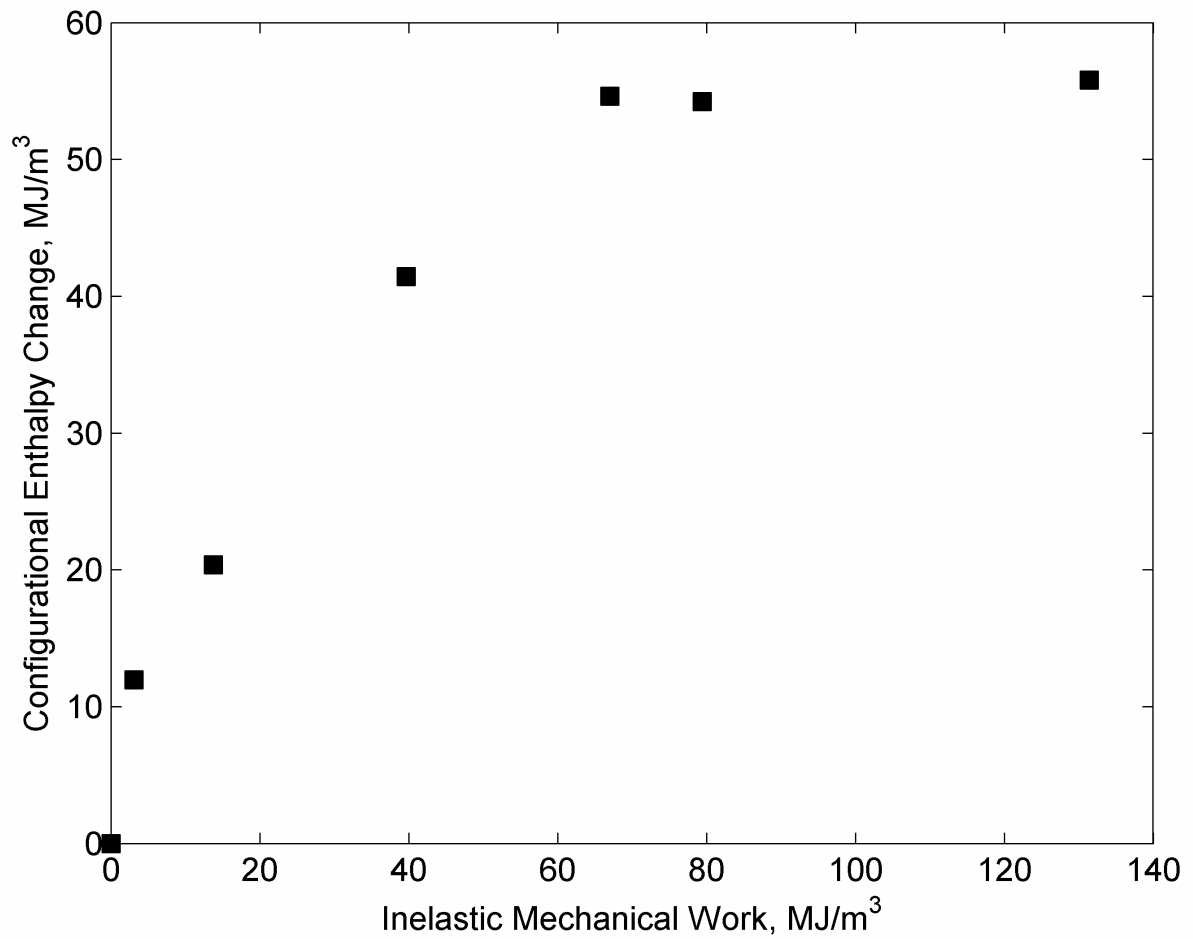


**Figure 6.4.** Configurational enthalpy for the quenched unloaded Pd<sub>43</sub>Ni<sub>10</sub>Cu<sub>27</sub>P<sub>20</sub> specimens as measured with Differential Scanning Calorimetry at a scan rate of 10 K/min versus inelastic mechanical work,  $W$ .  $W$  was calculated as the area under the curve for the stress strain diagrams, and was corrected for the elastic energy.

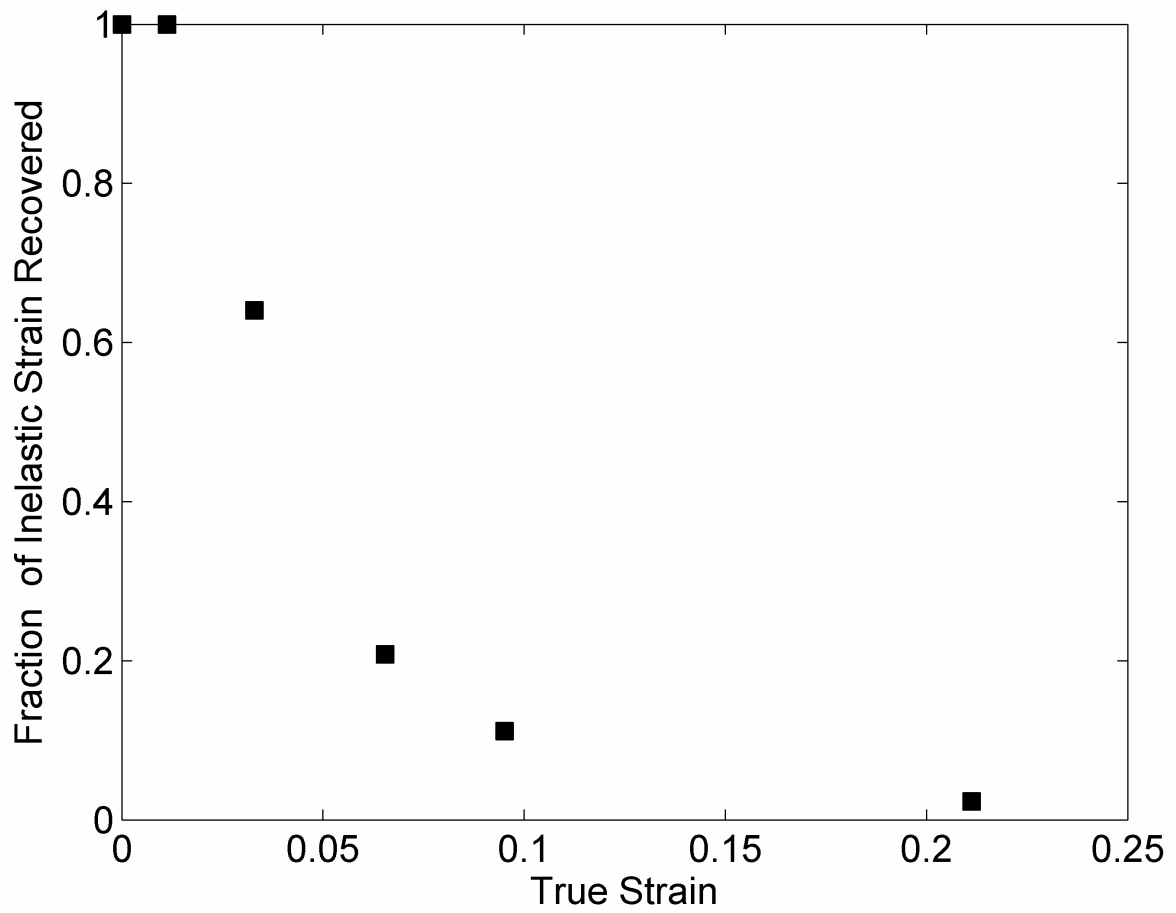


**Figure 6.5.** The time dependent anelastic recovery is plotted as a percentage of the total inelastic deformation of the specimen versus true strain. The anelastic recovery was accomplished by annealing at 558K for 4 hr.

by the surrounding glass matrix [13, 14]. If the external stress field is removed, and the specimen is allowed to relax, these mechanically polarized regions will relax to their original configurations, and the Eshelby stresses will be relaxed. This is what gives rise to the anelastic response seen in Fig. 6.5. The Eshelby stress fields associated with each  $\beta$  buckle up will tend to bias the surrounding glass in a way that will facilitate further  $\beta$  buckle ups in the surrounding region. As the external stress field is increased, the population of  $\beta$  buckle ups will increase. That population will continue to increase until the  $\beta$  buckle ups begin to cooperatively deform to eliminate the Eshelby stress fields, thus lowering the energy of the system, in what we will ultimately call the  $\alpha$  process. While the  $\beta$  buckle ups will be completely reversible, the  $\alpha$  process will correspond to a permanent irreversible plastic deformation. From this it may be assumed that the energy barrier for  $\alpha$  relaxation can be directly related to the Eshelby stress field. In steady state, the rate at which energy is stored in  $\beta$  buckle ups will be equivalent to the rate at which energy is dissipated in the  $\alpha$  process.

The competition between the two relaxation processes can be seen in Fig. 6.5. In the early stages of deformation everything is recoverable and the only process that has occurred corresponds to the  $\beta$  buckle ups. At larger total strains the fraction of recoverable anelastic strain decreases. If the  $\alpha$  process is a function of the  $\beta$  buckle up density, this would suggest that the density of  $\beta$  buckle ups initially increases during deformation until the rate at which the  $\alpha$  process occurs reaches the time scale of the experiment. As more  $\alpha$  processes occur, the density of  $\beta$  buckle ups will increase at a diminishing rate. Once a critical density of  $\beta$  buckle ups is reached, a kinetic balance

will be established with the  $\alpha$  process and any further deformation will become perfectly plastic and irreversible.

Figs. 6.6 and 6.7 show  $\Delta h$  and the flow stress in steady state at different strain rates. Both curves are observed to approach a limiting value at higher strain rates, and go to zero in the limit of infinitely slow strain rates. This corresponds to the transition from Newtonian flow, to non-Newtonian flow, and finally to shear localization. The change in  $\Delta h$  will be zero for Newtonian flow conditions. This is not shown in Fig. 6.6 because it was not possible to obtain Newtonian flow on the time scale of the experiments done. It is possible to describe the behavior seen in Figs. 6.6 and 6.7 using the  $\alpha$  and  $\beta$  relaxation processes described above. At slow strain rates the system is dominated by  $\alpha$  relaxations. This corresponds to having very few mechanically polarized regions in the material. At faster strain rates a steady-state balance between the storage of energy in the  $\beta$  buckle ups and the dissipation of energy in the  $\alpha$  relaxation is established. When the material reaches the shear localization regime energy is being stored in the  $\beta$  buckle ups faster than it can be dissipated in the  $\alpha$  relaxation. The result is that the material creates a shear band to dissipate the excess energy. At higher strain rates there will be a larger population of the mechanically polarized regions. This will result in higher flow stresses and larger changes in configurational enthalpy. Conversely at slow strain rates the population of mechanically polarized regions is smaller and lower-flow stresses and smaller changes in configurational enthalpy are observed. Just prior to shear localization the material should be ideally plastic, and all points on the potential energy landscape should be equally populated. Hence, the measured configurational enthalpy just prior to shear localization should correspond to half the barrier height controlling flow and its



value will be related to the density of  $\beta$  buckle ups and the associated Eshelby stress.

By looking at these limiting values it should be possible to probe the barrier to activate flow.

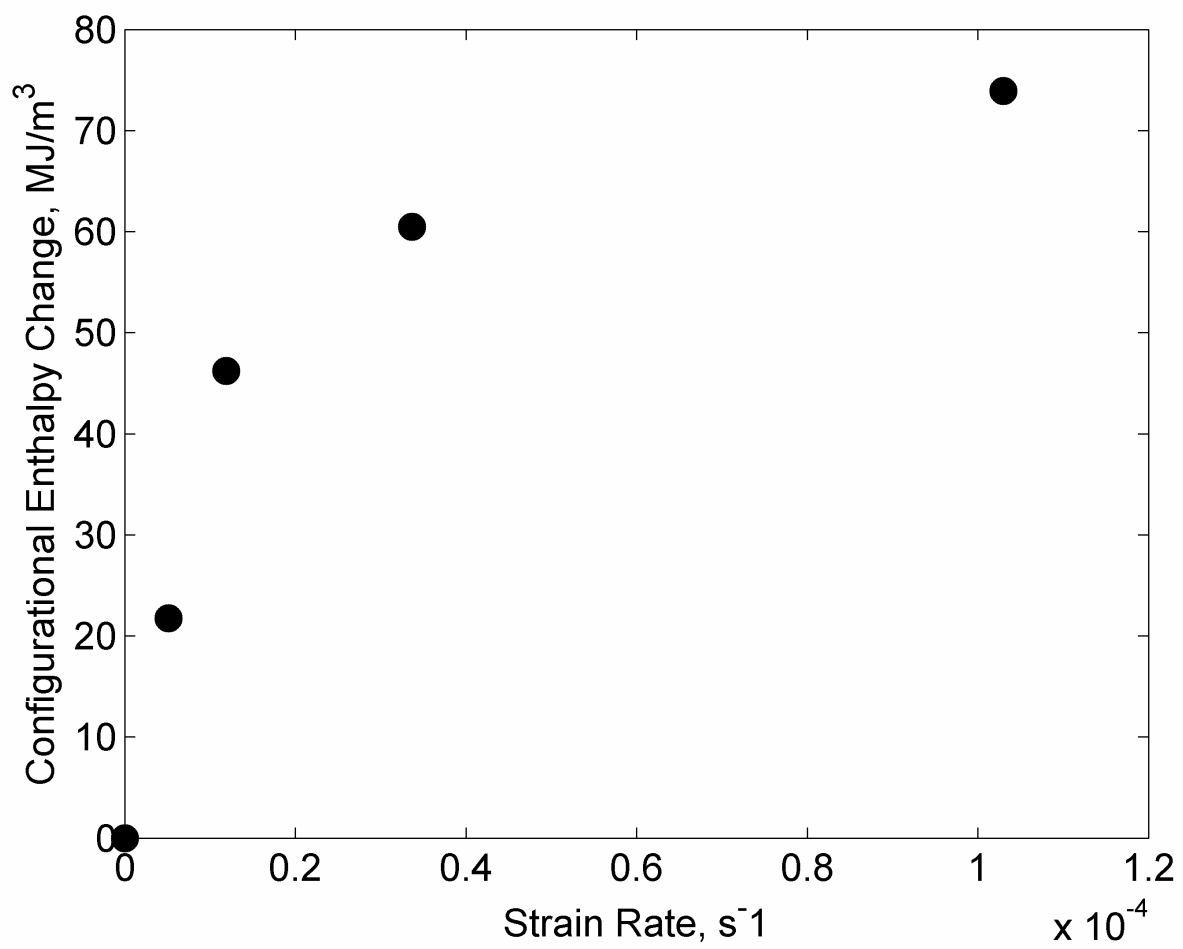


**Figure 6.6.** The change in steady state configurational enthalpy for samples deformed at 548 K. The enthalpies are referenced to a sample relaxed at 548 K.

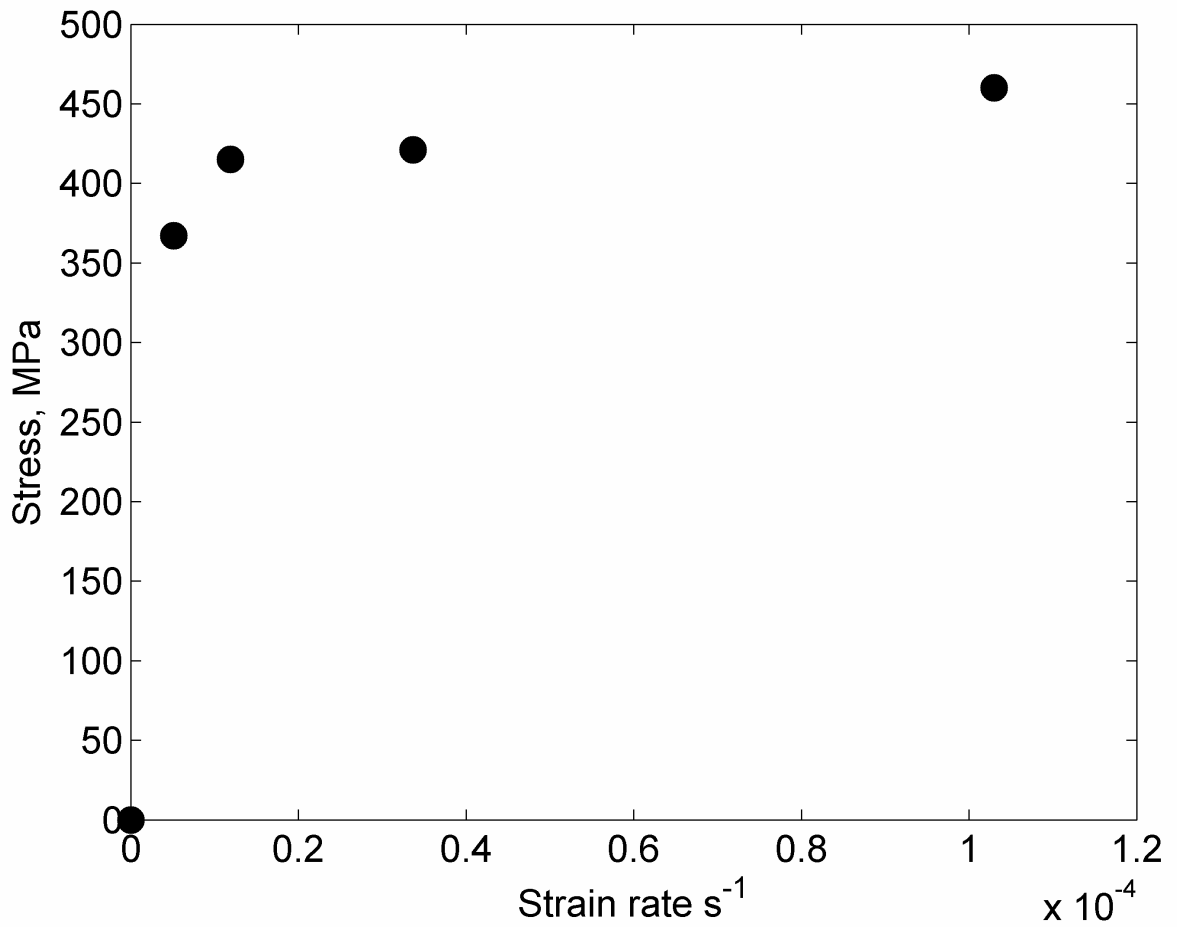


**Figure 6.7.** The steady state flow stress of the system as a function of the strain rate for samples deformed at 548 K

## 6.5 Conclusion

In conclusion the transient deformation regime was investigated by measuring the configurational enthalpy, isoconfigurational shear modulus, and the anelastic recovery through steady-state. The results from these tests identified an efficient conversion of input mechanical work into stored configurational enthalpy through steady state. In steady-state deformation the system transitioned to a completely dissipative process. The isoconfigurational shear modulus was found to decrease with increasing configurational enthalpy in agreement with the results in Chapter 5. The anelastic response accounted for the complete inelastic deformation of the system prior to the transient peak stress. Once the transient peak stress was reached a mixture of plastic and anelastic deformation was observed. As the amount of total deformation increased, the percentage of anelastic deformation decreased.

The Cooperative Shear Model developed by Johnson and Samwer [15] and the mechanically polarized regions envisioned by Argon et. al. [10-12] were used in an attempt to explain the observed mechanical behavior. In conventional glassy materials there is a proposed anelastic  $\beta$  response that is completely recoverable and an irreversible  $\alpha$  relaxation. In the current chapter the  $\beta$  response as applied to metallic glasses is described in terms of a  $\beta$  buckle up that is a mechanically polarized region within the glass. Furthermore, the mechanically polarized areas will be subject to an Eshelby stress, and it is that Eshelby stress that gives rise to the anelastic behavior of the material. In this description as the  $\beta$  buckle up density increases, the  $\beta$  buckle ups will begin to cooperatively deform to relieve the Eshelby stresses in a dissipative  $\alpha$  process.

By looking at the responses of the system to different strain rates approaching the shear localization strain rate it was possible to probe the criteria for forming a shear band and the barrier controlling flow. At a constant deformation temperature and an increasing strain rate both the steady-state flow stress and the steady-state configurational enthalpy appear to go to constant values. When the rate at which energy is input into the system exceeds the dissipative ability of the material at a given temperature the glass will shear localize in an attempt to lower the energy of the system. The total energy stored in  $\beta$  buckle ups at strain rates just prior to shear localization should be roughly equal to half the barrier height controlling flow. Additionally, the  $\beta$  buckle ups are areas of increased stress and will be involved in determining the absolute value of the flow stress. Furthermore, the stress and the energy stored in individual  $\beta$  buckle ups will be related to the Eshelby stress field. Therefore, it should be possible to relate the density of  $\beta$  buckle ups and the value of the Eshelby stress to the barrier controlling flow for the system and the flow stress prior to shear localization.

## 6.6 References

- [1] J. Hodowany, G. Ravichandran, A. J. Rosakis, and P. Rosakis, *Experimental Mechanics* 40, 113 (2000).
- [2] H. A. Bruck, A. J. Rosakis, and W. L. Johnson, *J. Mater. Res.* 11, 503 (1995).
- [3] S. Capaccioli, and K. L. Ngai, *J. Phys. Chem. B* 109, 9727 (2005).
- [4] G. P. Johari, and M. Goldstein, *J. Chem. Phys.* 53, 2372 (1970).
- [5] J. P. Johari, G. P. Power, and J. K. Vij, *J. Chem. Phys.* 117, 1714 (2002).
- [6] G. P. Johari, *J. Non-Crystalline Solids* 307-310, 317 (2002).
- [7] E. Orowan, "Creep in Metallic and Non-Metallic Materials," *Proceedings of the First U.S. National Congress of Applied Mechanics, A.S.M.E.*, 453,(1952).
- [8] O. P. Bobrov, K. Csach, S. V. Khonik, K. Kitagawa, S. A. Lyakhov, M. Yu. Yazvitsky, and V. A. Khonik, *Scripta Mater.* 56, 29 (2007).
- [9] A. Concustell, J. Sort, A. L. Greer, and M. D. Baro, *Appl. Phys. Lett.* 88, 171911 (2006).
- [10] A. S. Argon, *Acta Metall.* 27, 47 (1979).
- [11] A. S. Argon, and H. Y. Kuo, *J. Non-Crystalline Solids* 37, 241 (1980).
- [12] A S Argon, and L T Shi, *Acta Metall.* 31, 499 (1983).
- [13] J. D. Eshelby, *Proc. R. Soc. A* 241, 376 (1957).
- [14] J. D. Eshelby, *Prog. Solid Mech.* 2, 89 (1961).
- [15] W. L. Johnson, and K. Samwer, *Phys Rev. Lett.* 95, 195501 (2005).
- [16] M. L. Lind, G. Duan, and W. L. Johnson, *Phys. Rev. Lett.* 97, 015501 (2006).
- [17] M D Demetriou, J S Harmon, M Tao, G Duan, K Samwer, and W L Johnson, *Phys. Rev. Lett.* 97, 065502 (2006).

- [18] J S Harmon, M D Demetriou, M Tao, and W L Johnson, *Appl. Phys. Lett.* 90, 131912 (2007).
- [19] N Nishiyama, and A Inoue, *Mat. Tran. JIM* 37, 1531 (1996).
- [20] J Lu, Ph.D. Thesis. Pasadena: California Institute of Technology (2002).
- [21] E. Schreiber, O. Anderson, and N. Soga, Elastic Constants and their Measurement, New York: McGraw-Hill (1973).
- [22] P. Tuinstra, R. A. Duine, J. Sietsma, and A. van den Buekel, *Acta Metall. Mater.* 43, 2815 (1995).
- [23] G. Duan, M.L. Lind, M.D. Demetriou, W.L. Johnson, W.A. Goddard III, T Cagin, and K. Samwer, *Appl. Phys. Lett.* 89, 151901 (2006).